



A Realization of the SI Watt by the NPL Moving-coil Balance

To cite this article: B P Kibble *et al* 1990 *Metrologia* **27** 173

View the [article online](#) for updates and enhancements.

You may also like

- [Exhibition of Monogamy Relations between Entropic Non-contextuality Inequalities](#)
Feng Zhu, , Wei Zhang et al.
- [The watt or Kibble balance: a technique for implementing the new SI definition of the unit of mass](#)
Ian A Robinson and Stephan Schlamming
- [Data and analysis for the CODATA 2017 special fundamental constants adjustment](#)
Peter J Mohr, David B Newell, Barry N Taylor et al.

A Realization of the SI Watt by the NPL Moving-coil Balance

B. P. Kibble, I. A. Robinson and J. H. Belliss

National Physical Laboratory, Teddington, Middlesex TW11 OLW, United Kingdom

Received: March 8, 1990

Abstract

Mechanical and electrical power in SI units have been equated by measurements made on a coil part of which is in a strong magnetic field. The force due to a current I flowing in the coil, is weighed by opposing it with a mass M subject to the earth's gravitational acceleration g . This is combined with a separate measurement in which a voltage V is generated in the coil when it is moved vertically with velocity u through the relationship

$$IV = Mgu.$$

If the current produces a voltage V across a resistor whose value R is known in SI units [1], then

$$V = (MguR)^{1/2}.$$

Hence the voltage V and the current I are known in SI units and can be used to express the value of the NPL working standards in SI units. The working standard of voltage has hitherto been maintained in terms of a Josephson effect apparatus by ascribing the value 483 594 GHz/volt (maintained) to the Josephson constant K_J , presumed equal to $2e/h$ [2]. The measurements reported here suggest a different value of K_J 483 597,903 \pm 0,035 ought to be used, based on the premise that the SI value of the quantum Hall resistance is $R_K = 25\,812,8092 \pm 0,0014 \, \Omega$ [3].

If one presumed also that $R_K = h/e^2$ exactly, the values of elementary charge e and the Planck constant, h , [4] which may be deduced from these measurements are

$$e = 1,602\,176\,35 \pm 0,000\,000\,14 \times 10^{-19} \text{ C},$$

$$h = 6,626\,068\,21 \pm 0,000\,000\,90 \times 10^{-34} \text{ J s},$$

which may be compared with the values recommended by the CODATA Task Group on Fundamental Constants [5] which are

$$e = 1,602\,177\,33 \pm 0,000\,000\,14 \times 10^{-19} \text{ C},$$

$$h = 6,626\,075\,5 \pm 0,000\,004\,0 \times 10^{-34} \text{ J s}.$$

1. Introduction

1.1. Purpose of the Measurement

Two electrical units need to be obtained in terms of the base SI units of mass (the prototype kilogram), length (the metre) and time (the second) in order to ensure that consistent SI units are available for electrical measurements so that, for example, electrical and mechanical power are equivalent. The unit of resistance and impedance, the ohm, causes little difficulty as it can be realized from a calculable capacitor in terms of the metre and the defined values of the velocity of light and magnetic permeability of free space to just about sufficient accuracy ($\approx \pm 1$ in 10^7) to satisfy present needs. The other electrical unit to be so determined has formerly been the ampere, by using some form of current balance, but the uncertainty of a few parts in 10^6 was far larger than that now required. Apart from the scientific need of those who seek for inconsistencies in the interconnected network of values of the fundamental physical constants, commercial voltage standards and voltage measuring instruments having less than one part in a million (ppm*) uncertainty must be calibrated. To meet the second requirement it has been expedient to use a maintained representation of the volt which was believed to be equal in magnitude to the SI volt (to within the realization error of the latter) by ascribing an arbitrary numerical value to the conversion factor for the ratio of frequency to voltage occurring in the ac Josephson effect. A voltage standard based on this phenomenon is capable of providing a voltage reproducible to 1 part in 10^8 in terms of this conversion factor. Therefore it is timely to determine more accurately a representation of the volt in SI units so as to place the electrical units on a sound SI footing.

1.2. Principle of the Measurement

The NPL apparatus, which realizes the electrical watt, measures the force produced when a current I flows

* 1 ppm $\equiv 1 \times 10^{-6}$

through a coil suspended from a balance so that the coil lies partly in the field of a large permanent magnet. This force is balanced by a mass M subject to the earth's gravitational acceleration g [6].

In a separate measurement the coil is moved vertically with velocity u and the emf V induced in it is measured. Equality of the units of mechanical and electrical power implies that

$$IV = Mgu.$$

If V is made equal to the potential difference across a resistor carrying the current I whose value R is known in SI ohms from a calculable capacitor determination, then the voltage V in SI units is given by

$$V = (MguR)^{1/2}.$$

Neither the dimensions of the coil nor the flux density and distribution of the magnetic flux need be measured. Moreover, the only length measurement required is that needed to establish the velocity u , and this is observed as a part of the measurement in contrast to the determination of the dimensions of current balance coils which are measured at another time and place from that of their use to determine the ampere.

In principle, instantaneous values are required for u and V as the coil passes through the weighing position, but in practice the magnetic flux and coil can be so shaped that V/u is almost constant and an average over a finite distance is adequate.

An apparatus built to embody the above principles can be designed [7] so that the magnitudes of the observables involved are suitable for accurate measurement. In the apparatus to be described in detail below, a current of 10 mA flowing in a coil of 0,25 m mean width having 3362 turns immersed in a magnetic flux density of 0,7 T generates 1 kg weight change of force when the current is reversed. The current also flows through a standard 100 ohm resistor and the 1 volt potential drop produced across it is compared with a standard voltage source. When the coil is moved through the magnetic flux at 2 mm/s, corresponding to the passage of about 6000 optical fringes per second in the interferometer, 1 volt is generated in it and again compared with the voltage standard. The current, the force, the voltage and the velocity are all capable of being observed with 0,1 ppm resolution or better.

One difficulty is caused by the presence of ground vibrations at the experimental site. This site, although moderately good, still suffers vibrations with peak velocities of the order of $1 \mu\text{m/s}$, which is 5×10^{-4} of the velocity to be observed, and superimposes a random component of this magnitude on it. Although our apparatus incorporates a servo-control to regulate the mean velocity of the coil to within about 10 ppm, because of the various mechanical resonances of the coil-balance system it is difficult to design the feedback to give a servo-control of sufficient gain and bandwidth to overcome these vibrations. Fortunately, this is not necessary. Since the instantaneous values of voltage and velocity are proportional, if the mean voltage and velocity over the same time interval are observed their ratio will be independent of their fluctua-

tions. We observe the mean velocity as the displacement occurring over the time interval during which the mean voltage is measured as the output of a calibrated integrator. In this way the effect of vibration is almost eliminated and the resulting standard deviation of the V/u data is 0,1 ppm or less.

2. The Apparatus

The mechanical aspects of the apparatus have remained virtually unchanged during the period of all the measurements reported here. The interferometer and the digital and analogue control and measurement system were simplified in 1987, and only this improved version is described here.

2.1. Overall View

The coil shown in Fig. 1 is constructed from two approximately square coils of square cross-section joined together mechanically and connected electrically so that the

conducting path is as . Ambient 50 Hz flux threads

both halves approximately equally, and therefore does not induce any significant overall emf, yet the coil responds fully to the passage of the central limb through the localised flux of the magnet. The coil is shown edgewise on in Fig. 2 between the pole-pieces of a large permanent magnet. The coil is suspended from the balance, and on the floor of the balance case, coaxial with the suspension column, is an auxiliary magnet assembly. An auxiliary coil is attached to the column so that it is within the magnet gap. The whole assembly has a similar geometry to a loudspeaker coil and magnet. Currents supplied to this auxiliary coil drive the suspended coil along a vertical axis when required.

The balance case is supported on a hydraulically-lifted shaft attached to the side of the magnet which provides a vertical bearing about which the balance case can be rotated to assist alignment of the coil in the gap. It also provides a means of lifting balance and coil with respect to the magnet so that weighings can take place with the coil occupying positions along its almost vertical trajectory when it moves. The whole apparatus is massively constructed to achieve stiffness against vertical accelerations and minimize the vibrational difficulty outlined in Sect. 1.2. The coil weighs about 30 kg and the balance beam about 40 kg so that about 100 kg weight bears on the central knife-edge of the balance.

The arrangement for measuring the current which, when reversed, opposes the force due to the lowering of a mass M is outlined in Fig. 3a. The reading of the laser interferometer which corresponds to the balance beam being horizontal having been determined, departures from this reading are registered by the computer which adjusts the output of a programmable current source to restore equilibrium. The equilibrium current I is measured in terms of the potential drop it produces across a

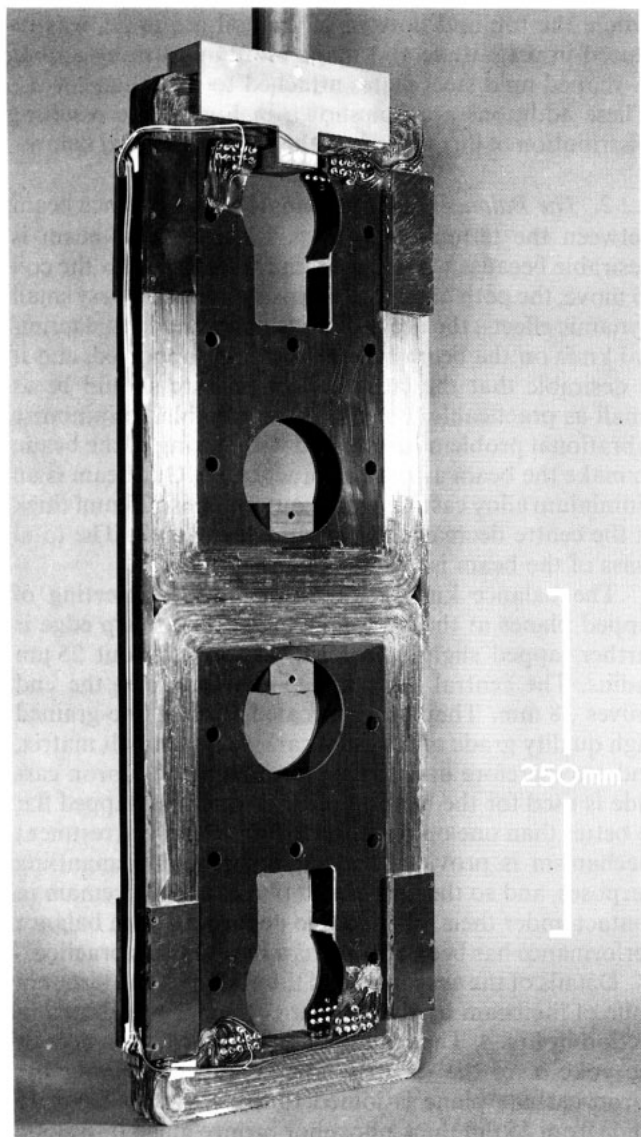


Fig. 1. The coil

standard resistor R , and this potential is in turn measured as the small difference between it and the voltage V of a standard source recorded by an integrating voltmeter interfaced to the computer. The mass M is then lowered, the current I assumes an approximately equal and opposite value and is again measured, the reversing switch having been operated to reverse the sense of V .

The arrangement for the measurement of the voltage generated in the moving coil is shown in Fig. 3b. The motion of the coil is sensed by the passage of optical fringes through the laser interferometer [8]. These are compared with a fixed 6 kHz frequency obtained by dividing 384 kHz by 64. Use of a multiple of the required frequency enables the comparator circuitry [9] to obtain phase information to $1/64$ of a cycle. Any phase discrepancy is corrected by a current fed to the drive coil and magnet D. The velocity kept constant in this way is measured by the counter which is gated to operate over the interval during which the integrating voltmeter is recording the integrated difference between the voltage generat-

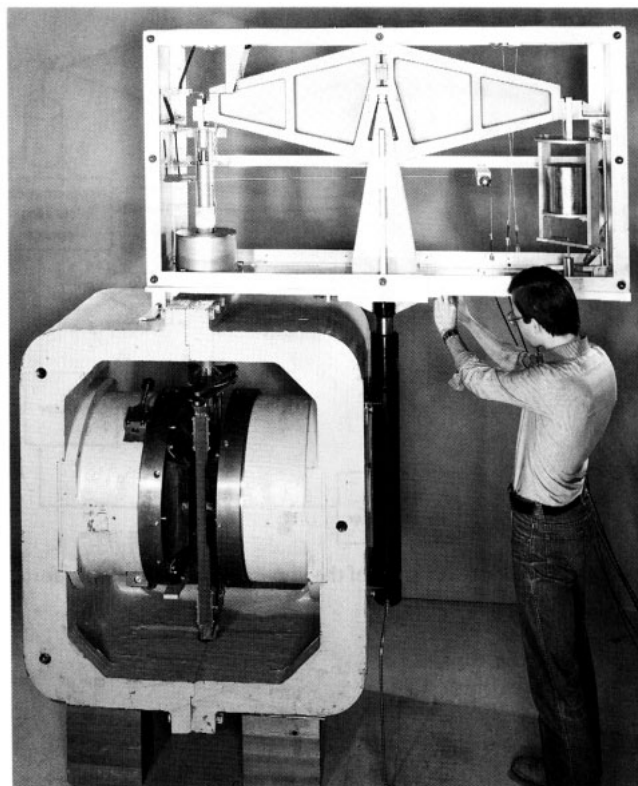


Fig. 2. The coil suspended from the balance beam so as to be in the magnetic flux of the large permanent magnet. The auxiliary magnet assembly containing the drive coil is at the bottom left of the balance case; above it is the mechanism which limits the balance travel during weighing and the mass and scalepan in the centre of the vertical column. A hydraulic ram to lift the whole balance is fixed to the right-hand side of the magnet

ed by the coil and that of the standard V . After traversal in the upwards direction, the motion of the coil is reversed and the voltage generated again compared with V , whose sense has been changed with the reversing switch.

Because in both the weighing and the traversal measurements the sense of the voltage measured and of the standard are reversed, any real or apparent voltage sources such as thermoelectric emf's in the circuit or offset of the integrating voltmeter are eliminated by taking the mean of the forward and reversed measurements.

2.2. Detailed Description

2.2.1. The Magnet.

The permanent magnet is of massive construction, and weighs about 6000 kg. The 0,1 m thick mild steel yoke provides considerable low-reluctance and eddy-current shielding against the penetration of both static and time-varying magnetic fields into the air-gap. Nevertheless, sources of 50 Hz fields such as instrument transformers, motors etc. are kept remote from the magnet. The Columax permanent magnetic material between the yoke and the pole-faces provides a 0,68 T flux density in a 56 mm gap between the $0,3 \times 0,3$ m square pole-pieces which are lapped optically flat. The magnetization process [10] involves a final decrease in the flux density to leave the magnet immune to ageing

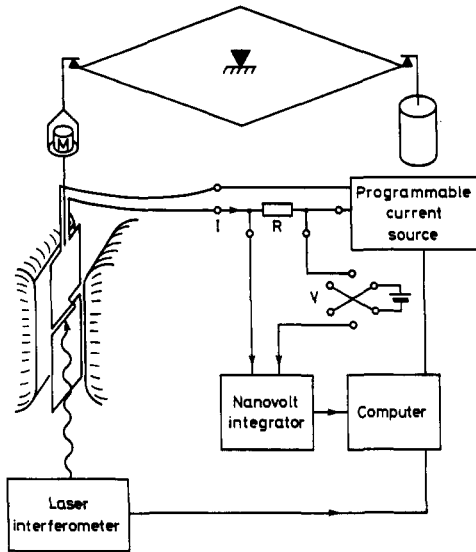


Fig. 3a. A schematic diagram of the apparatus as arranged for force measurement

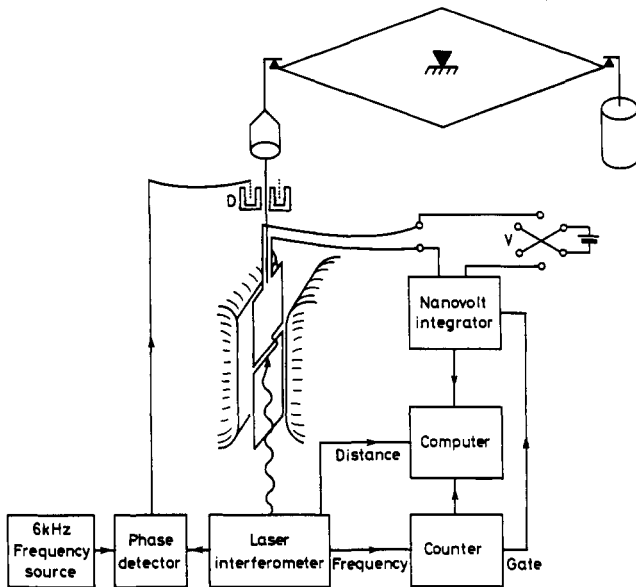


Fig. 3b. Arranged for V/u measurement

effects. The temperature coefficient of the flux density is about 200 ppm/ $^{\circ}\text{C}$. The magnet rests on four wooden blocks (for thermal isolation) on a solid concrete raft laid directly on the sub-soil. Packing under the blocks and the rotational adjustment about a horizontal axis in the field direction with which the polefaces are provided enabled the field direction to be adjusted to be horizontal within 10^{-4} rad and the top and bottom field boundaries to be horizontal. The method of measuring this horizontal field condition using a galvanometer movement is described in reference [11]. Movement of one pole-piece in a vertical plane with respect to the other enabled a high degree of symmetry of the field pattern about a vertical plane midway between the polepieces to be achieved. The field in the regions between the pole-pieces and the magnet yoke,

where the top and bottom of the coil are to lie, was reduced in magnitude and made more uniform by adding L-shaped mild steel plates attached to the magnet yoke. These additions are not shown in Fig. 2. The resulting distribution of flux threading the coil is discussed below.

2.2.2. The Balance. The total length of the balance beam between the terminal knives is 1.2 m. A long beam is desirable because when the beam rotates to allow the coil to move, the path of the coil is closely (ignoring very small dynamic effects) the arc of a circle described by the terminal knife on the beam from which it is supported, and it is desirable that the curvature of this arc should be as small as practicable. But it is also desirable, to minimize vibrational problems associated with flexing of the beam, to make the beam as rigid as practicable. Our beam is an aluminium alloy casting whose outer web is 125 mm thick at the centre decreasing to 60 mm at the ends. The total mass of the beam is about 44 kg.

The balance knives are formed by the meeting of lapped planes at the traditional 120° . The sharp edge is further lapped slightly to form an arc of about $25\ \mu\text{m}$ radius. The central knife is 125 mm long and the end knives 38 mm. They are fabricated from a fine-grained high quality grade of tungsten carbide in a cobalt matrix, and are therefore undesirably ferromagnetic. Boron carbide is used for the bearing planes, which are lapped flat to better than one optical fringe. Only a crude arrestment mechanism is provided for alignment and dismantling purposes, and so the knives and planes usually remain in contact under their full load. No deterioration in balance performance has been noticed as a result of this practice.

Details of the suspension of the coil from the terminal knife of the beam by the tubular column T are shown in section in Fig. 4. The column T passes through a hole in the yoke Y of the magnet. The stirrup containing the boron carbide plane is joined to T by a strip hinge H made from $25\ \mu\text{m}$ thick phosphor bronze glued into slots. This strip hinge gives flexibility of the support in a direction perpendicular to the knife-edge so that the centre of the force on it must pass through a definite point vertically above H. In orthodox accurate balances it is usual to provide additional flexibility in the plane of the knife, for example by a second strip hinge perpendicular to H, so that the knife does not take up different rotational orientations with positioning of masses on the pan below, but in our case this is unnecessary because the 30 kg dead mass of the coil keeps the supporting column sufficiently vertical. Also, the force due to current reversal in the coil and its opposition by a carefully centred mass M are directed very closely along the axis of the suspension. The centre of mass of the coil is on this axis. The parallel sides of the coil are adjusted to be approximately vertical by bending the supporting column at flexure hinges acting in two perpendicular horizontal axes. These hinges are made by cutting slots in the supporting tube as shown in the lower inset to the diagram and flexed by means of four screws S (the two giving the perpendicular motion are not shown) which bear on a rod up the axis of the tube with its lower end fixed rigidly into the coil supporting harness D.

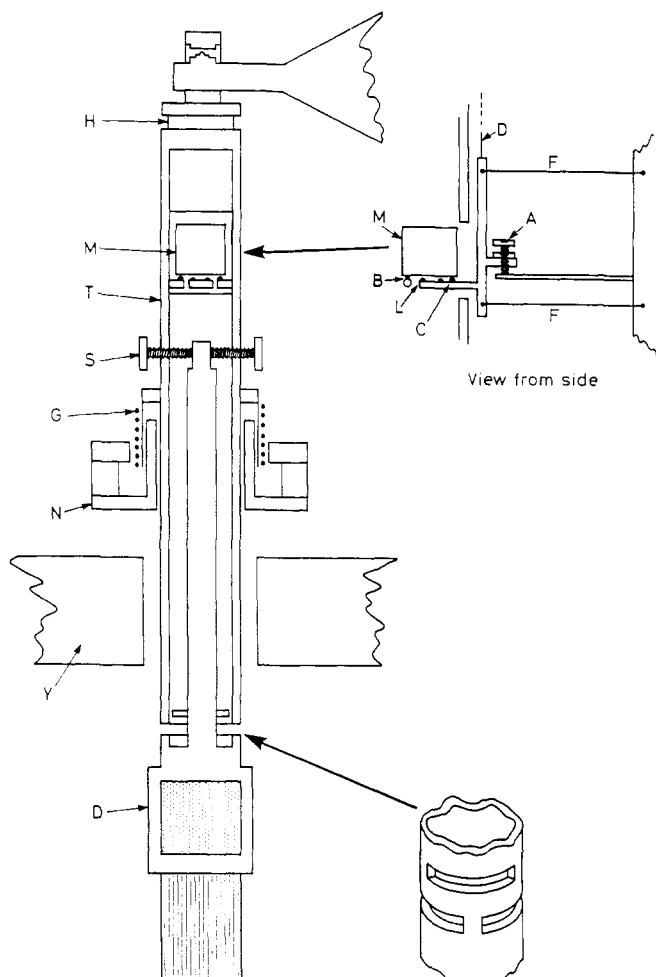


Fig. 4. A section through the column suspending the coil. This shows the mass raising and lowering arrangement, the drive coil and magnet, and the adjustment for placing the centre of mass of the coil on the axis of the column

The mechanism for raising and lowering the mass *M* is shown in more detail in the section (as seen from a perpendicular direction) in the upper inset. Mass *M* is on a pan-plate, except in the case of a 1 kg mass when none is necessary, and this or the kilogram rests on four precision phosphor-bronze balls 3 mm in diameter inset at the end of four short rods which protrude into the bore of the supporting tubular column. It can be lifted off by raising the cantilever *C*, which is provided with four similar balls, up between the rods by pulling on the flexible, non-magnetic wire *D*, motion being allowed by the long strip-hinges *F*. On lowering again, the rest position of *C* is determined by the adjustable stop *A*. Two movements are provided for *D*, a fine movement to raise *C* far enough just lift *M*, and a larger one to lift *M* further and allow the ± 25 mm movement needed for measurement of the voltage generated from the moving coil.

The centre of gravity of the balance beam can be adjusted to be at the same height as its central knife-edge by raising or lowering the brass masses on the screwed rods seen in the centre of the beam in Fig. 2. This adjustment was initially done by making the periodic time of the balance very long, but a later, more critical, adjustment was carried out by observing the near-zero current

in the coil needed to keep the balance in equilibrium (without any opposing force from lowered masses) as a function of the equilibrium angle of the beam to the horizontal. When correct adjustment was attained this current was independent of small rotations of the beam from horizontal.

Despite this adjustment, it is nevertheless crucial to the accuracy of determining the magnitude of the vector force of interaction of a current and the magnetic field by opposing it with a mass subject to gravity that this opposition be carried out with the balance beam as closely horizontal as possible. If the plane containing the knife-edge supporting the coil and the central knife is not horizontal, any horizontal component of the force on the coil in the plane of the balance beam will exert a couple on it and cause a systematic error. By a procedure outlined in the following section, the coil is aligned with respect to the magnetic flux threading it so as to make this component as small as possible. The remaining error caused is then the product of two small quantities and can be made negligible. Verification of this is discussed in Sect. 3.3.2. The three knife-edges on the beam were set to be coplanar at the time of manufacture and the central bearing plane was set to be horizontal, and so it is necessary to find the condition for which the line joining the centres of the two end knife-edges is horizontal. This is done using a straight-edge incorporating a bubble level. The ends of the straight-edge are adjusted to be at the level of the end knives, and the horizontal condition of the beam is registered by an optical system consisting of a mirror attached to the beam reflecting light from a fixed source onto a pair of opposed photocells. Subsequently a signal from these photocells signals to the controlling computer that the balance beam is horizontal to a tolerance of about 5×10^{-4} rad.

The counterweight for the coil, shown on the right of Fig. 2, is made as a solid lead mass and an empty sealed can. Their total volume is calculated to be equal to that of the coil and its supports on the left of the balance so that changes in the ambient air density do not cause significant imbalance during a set of observations. The additional counterweight needed to oppose the force due to the current flowing in the forward direction is provided by a mass lowered on to the right-hand pan assembly by the mechanism shown in Fig. 5. Fine adjustment of balance equilibrium with no current flowing can be accomplished (without any need to open up the balance case) at the beginning of each day's work by adding or removing wire masses folded into a tetrahedral form. These are handled with a tool made from 1 mm wire inserted through a self-sealing hole in a small rubber insert in the front of the balance case.

The aluminium alloy balance case is constructed from 3 mm thick panels bolted to a girder framework on a 12 mm thick base-plate. For ease of handling, the removable front panel is a light-weight sandwich of 1 mm thick sheets with expanded foam plastic between them. The whole case is covered by 50 mm thick foamed plastic thermal insulation, the object being to ensure that the inside surfaces of the balance case are isothermal to prevent the setting up of perturbing convective air currents.

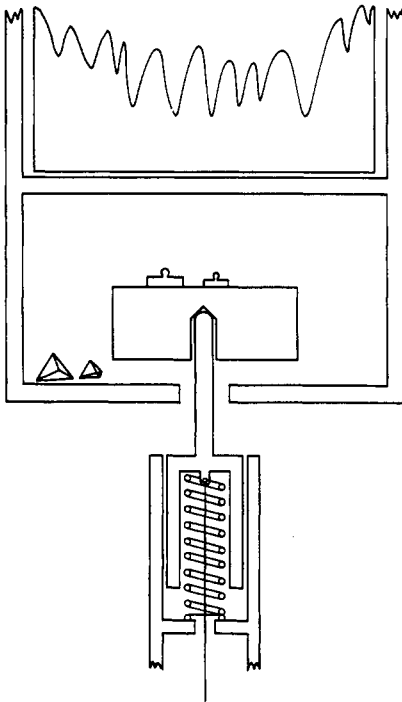


Fig. 5. The arrangement for raising and lowering the right-hand mass, and the small tetrahedral masses

2.2.3. The Coil and its Alignment in the Magnetic Field.

The coil assembly is shown in Fig. 1. It consists of two identical coils on skeletal tufnol formers glued together, with additional tufnol strips glued down each side of the assembly to form a rigid whole. The corner-cube for the interferometer is embedded in the tufnol block visible in the top of the circular aperture in the lower coil former. A similar dummy block in the upper former preserves symmetry and provides the option of inverting the coil assembly if required.

The windings of each coil consist of 41 turns of a ribbon of 41 wires of enamelled copper wire of 0,97 mm overall diameter. The coil formers were provided with temporary side cheeks and successive layers were coated with a quick-setting epoxy glue and then pressed into place. The completed coils were very rigid and moderately precise, with corresponding wires on opposite sides parallel to better than 10^{-3} rad. After the insulation between them had been tested, the 41 side-by-side pancake sections of each coil were connected in series to give 1681 turns. The two coils of the assembly were then connected in series to give a final total of 3362 turns. The total coil resistance was about 100 Ω .

Connection to the coil was made by insulated conductors going up the supporting column to a terminal block at its top and thence by 0,012 mm diameter bare wires in a loop to a similar block on the balance beam. Further conductors went along the beam to the vicinity of the central knife where a similar system of terminal blocks and flexible wire loops conveyed the connections to the balance support and case and thence to the rest of the electrical measuring system. The fine wires are only required to flex through a small angle with rotation of the beam and end-knife and therefore exert a very small and

constant torque which does not affect the accuracy of the force measurement.

The coil needs to be aligned with respect to the magnetic field so that the flux Φ threading it only changes with vertical (x) movement of the coil, and not with horizontal movements in either the direction of the field (z) or in the perpendicular direction (y), or with possible torsional motion about its vertical axis.

The total emf induced in the coil is given by

$$-V = \partial\Phi/\partial x \cdot dx/dt + \partial\Phi/\partial y \cdot dy/dt + \partial\Phi/\partial z \cdot dz/dt$$

whereas the vertical component of the force on the coil with current I flowing in it is

$$F_x = -I \partial\Phi/\partial x,$$

whence,

$$V = u F_x / I - \partial\Phi/\partial y \cdot dy/dt - \partial\Phi/\partial z \cdot dz/dt.$$

Because of the symmetry of the field about the vertical axis and the near-vertical motion of the coil (it actually follows a path which is a short arc of a circle of radius equal to the half-length of the balance beam, and the path is vertical as the coil passes through the position it occupies for the force measurement), the second and third terms are negligible. This important matter was tested experimentally, as described in Sect. 3.3.1.

To ensure that any pendulum or torsional motion of the coil as it travelled vertically induced no additional voltage, as a routine alignment procedure, the balance beam was clamped in its horizontal position and these three motions made to occur in turn. The consequent voltages induced in the coil were observed with an oscilloscope, using a low-pass filter to eliminate voltages induced by rapid vertical vibrations. Rough adjustment was carried out by altering the position of the coil in the magnet gap, using the motions incorporated for this purpose in the balance case mounting. Final fine adjustment was accomplished by adjusting the position of small steel pieces in the fringing field of the magnet near to the vertical sides of the coil. The optimum adjustment could be detected with great sensitivity by observing when the sinusoidal voltage induced by the pendulum motion of frequency f of the coil consisted solely of a component at $2f$, denoting a symmetrical motion about the desired condition.

This alignment procedure does not ensure vanishing of the second and third terms of the above expression, as pendulum motion involves rotation of the coil as well as y - and z -translation, but it does ensure that the periodic voltages thus induced are negligible, as well as being averaged to zero by choosing the integration time to be equal to the periodic pendulum time. To ensure that the pendulum motion does not superimpose apparent periodic variations on the vertical motion of the coil, which would be registered by the interferometer, the optical centre of the corner-cube fixed to the coil should coincide with the centre of mass of the coil to within 1 mm. This adjustment was made by again clamping the balance beam and testing whether pendulum motion causes passage of interferometer fringes with periodicity f . Small additional

non-conducting masses were added as needed to the coil until only $2f$ variation was observed.

2.2.4. The Masses. The principal mass used for the 1,022 kg weighings is a platinum-iridium 1 kg cylinder manufactured at the International Bureau of Weights and Measures (BIPM) and coded 651. Its volume (for air buoyancy corrections) and mass were determined at the BIPM and its mass subsequently at the NPL in terms of the national standard kilogram and two other similar standards A and B. Because an unexplained 0,1 mg change occurred in the initial stages of our use of this mass, the NPL calibrations are the relevant ones, and are listed with dates in Table 1. Mass kg 18 was itself calibrated in 1978 against standards traceable to the prototype kilogram as $1 \text{ kg} + 59 \mu\text{g}$ after cleaning, in 1984 as $1 \text{ kg} + 76 \mu\text{g}$ before cleaning and again in 1986 as $1 \text{ kg} + 64 \mu\text{g}$.

The 0,511 kg mass was principally composed of Parliamentary Copy V of the pound, a platinum-iridium cylinder engraved with P.C.V. The recent accurate determinations of its mass are also listed in Table 1.

The 100 gm mass and the lesser masses are the set used in the work described in [10]. The masses of the whole set were measured in 1975 and 1986 at the NPL when the value of the 100 gm mass was $99,987\,954 \text{ g} \pm 10 \mu\text{g}$ and $99,987\,971 \text{ g} \pm 10 \mu\text{g}$. The 100 g mass only was measured in November 1984 when its mass was $99,987\,969 \text{ g} \pm 10 \mu\text{g}$ (95% confidence). The other masses were remeasured in January 1988, when negligible change was found from the 1986 measurement.

The aluminium alloy scalepan used with masses other than that of 1 kg was measured from time to time in terms of platinum-iridium masses. In air exhibiting only the normal variations of density, its apparent mass varies by at the most $\pm 30 \mu\text{g}$, and so, for simplicity, it was treated as if it were platinum-iridium, of this apparent mass.

2.2.5. The Electrical Measurement Circuit. The electrical measurement circuit is drawn in Fig. 6. The circuit and components are totally enclosed in a shield which has no loops and is connected to the low of the system only at the low input of the commercial digital voltmeter. This shielding ensures that the system is immune to the effects of external electric fields. The inter-component wiring is twisted wire-pairs, with equal and opposite currents in each member of the pair, and again there are no loops. This topology ensures freedom from voltages generated by external time-varying magnetic fluxes. The necessary power for the integrator, the solid-state standard voltage source and for the programmable current source are derived either from shielded battery packs or from totally isolated mains-powered supplies [12] whose properties with regard to external interference are virtually indistinguishable from the batteries contained within the screen. The digital information passed through the screen from the integrator to the current source goes via opto-isolators or fibre-optic cables whose transmitters and receivers are on opposite sides of the screen.

Good-quality insulating materials (predominately PTFE) are employed throughout and the total insulation from the system to screen is in excess of $10^{11} \Omega$. All

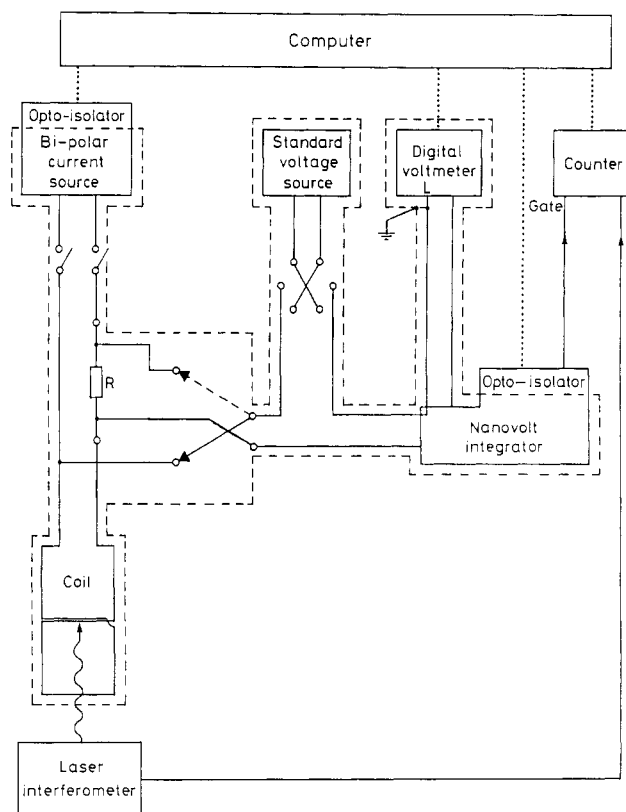


Fig. 6. The analogue electrical circuitry

Table 1. Masses of kg 651 and P.C.V.

Date	Mass/gm	Uncertainty (2σ)/ μg	Where measured
10. 80 and 9. 82	999,988 898	8	BIPM
12. 1983	999,988 924	8	BIPM
3. 1984	999,988 819	8	NPL
3. 1985	999,988 722	8	NPL
8. 1985	999,988 707	20	NPL
1. 1988	999,988 691	18	NPL
1960	453,592 138	15	NPL
1971	453,592 127	15	NPL
12. 1979	453,592 156	20	NPL
10. 1985	453,592 146	10	NPL
2. 1988	453,592 141	18	NPL

junction points in the potential-measuring part of the circuit use crimped copper terminations, copper binding screws or all-copper push-in connectors to minimize thermal emfs. Those thermal emfs that remain are almost negligible, but in any case are eliminated by the reversal of current and voltage in the two parts of the measurement.

It is important that the switch which reverses the connections to the standard voltage source exhibits very low thermal emfs as, otherwise, those which are not present when the standard voltage source is measured against the NPL maintained volt would cause a systematic error. Standard latching relays having silver-on-copper contacts were modified by drilling 0,3 mm diameter holes into the sides of the contacts, forcing in 0,3 mm copper

wire and centre-punching the vicinity of the hole to form a pressure-welded joint. When the relay contacts are closed, the thermal emfs measured between the wires are 5 nV or less. These modified relays have proved to be totally reliable. They are operated by circuitry powered by batteries within the shield, when commanded by optically-isolated pulses from the controlling computer.

2.2.6. The Standard Voltage Sources. Three standard voltage sources were used for the measurements reported here. One is a standard commercial solid state voltage reference made by Cropico Ltd. Its performance was improved considerably by placing it in a thermostated air enclosure whose temperature was regulated to within a few mK.

Our second standard voltage source is similar but constructed by P. Spreadbury. The chain of stable resistors which subdivides the Zener voltage was provided with taps to give three outputs, two, each nominally of 0,509 V, and the third, by connection across the outer taps, of 1,018 V.

The stability of the first of these solid-state sources over a few hours, which was the typical duration of a set of measurements, is illustrated in Fig. 7 where the measurement is shown relative to a stable Weston cell in a well-thermostated enclosure. It will be seen that the error in any observation made in terms of the solid state reference is not likely to be more than $\pm 0,05$ ppm if the solid state source is calibrated at some time during this period. The behaviour of the other source is very similar.

The third standard voltage source comprised commercial mercury batteries in an enclosure thermostated to better than 1 mK over 24 hours. Its voltage drifted at a constant rate of about 0,3 $\mu\text{V}/\text{hour}$ so that measurements made using it needed to be carefully timed, but its virtually noise-free output was an advantage. As it contained no semi-conducting devices its use was a test for the possible effects of noise rectification by the other sources.

The transfer of voltage to the NPL Josephson apparatus to 0,05 ppm accuracy presented many problems, and various strategies were tried during the course of these measurements. The most usual was to carry the portable thermostated Zener reference source to the

adjacent building where it was compared with a set of Weston cells, which were themselves periodically calibrated against a Josephson apparatus. Alternatively, the Zener reference source was compared directly against a Josephson apparatus. Some comparisons were carried out via a shielded, twisted conductor-pair cable routed between the buildings.

In 1985 the Josephson apparatus was a single-junction device whose voltage was scaled up with a calibrated resistive divider at liquid helium temperatures, using a SQUID as a null detector [13]. In 1987 this system was superseded by a Josephson array of junctions in series, capable of realizing a stable 1,018 V [14]. Comparisons carried out directly with this system were the most satisfactory, but for none of the measurements reported here did the error exceed $\pm 0,1 \mu\text{V}$. The actual uncertainty ascribed to this voltage comparison is assessed below.

2.2.7. The Standard Resistors. The standard resistors used are Wilkins-type class S standards made by Tinsley Ltd. A 100 Ω resistor is used for the measurements involving the kilogram mass (when the current involved is 10,18 mA), a 1000 Ω resistor for measurements involving the 100 gram mass (1,018 mA) and two 100 Ω resistors connected in series when 500 g of mass is used (5,09 mA). About 0,006 Ω of copper formed the link resistance between the resistors and the temperature coefficient of resistance of the combination is $+0,03$ ppm/K at 20 $^{\circ}\text{C}$. The temperature coefficients of all these resistors are sufficiently small that initially they were not thermostated. Instead they are thermally lagged and their temperature observed with a platinum resistance thermometer (placed electrically outside the shield), and a small correction made. The relevant properties of these resistors and their values in terms of the NPL realization of the SI ohm are given in Table 2. A linear drift rate of their value was assumed, as justified by the calibration data, and an interpolated value was used in the calculation of the result from each day's measurements. Their power coefficients were measured and found to be negligibly small in the present context.

For the 1988 results, the 100 Ω resistors were thermostated at about 22,6 $^{\circ}\text{C}$. Their temperature coefficients

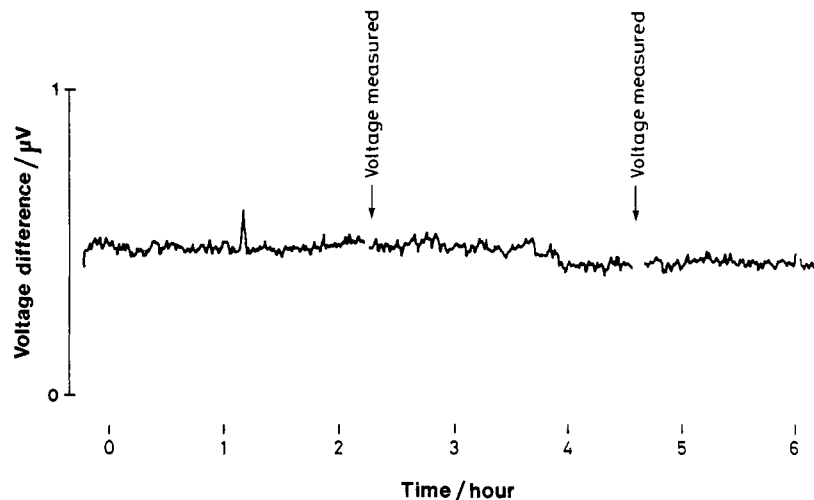


Fig. 7. The noise and short-term stability of the standard voltage source

were somewhat greater at this temperature, but resistance deviations caused by changes in the thermostated temperature were quite negligible. The values of the resistors and copper link were determined in 1987 and 1988 directly in terms of the quantum Hall apparatus [3].

2.2.8. Nanovolt Integrator. The circuit for the nanovolt integrator is shown in Fig. 8. An input voltage of up to 1 mV is amplified $\times 100$ by the low-noise, low-drift operational amplifier OP27 and then presented to the input of

Table 2. The resistors used for the measurements

Nominal resistance/ Ω Serial no. Manufacture date	Temperature coefficients **		Calibrated resistance/ Ω (at 20°C)	Date
	α /(ppm/K)	β /(ppm/K ²)		
100 222008 1974 (Thermostated at 22,6°C)	-0,13	-0,054	99,999 428	30. 4. 84
			99,999 443	19. 11. 84
			99,999 441	12. 3. 85
			99,999 448	21. 5. 85
			99,999 430*	16. 2. 87
			99,999 438*	15. 10. 87
			99,999 376*	2. 2. 88
100 222000 1974 (Thermostated at 22,6°C)	-0,03	-0,050	99,998 596	12. 3. 85
			99,998 603	21. 5. 85
			99,998 582*	15. 10. 87
			99,998 533*	2. 2. 88
			99,998 534*	1. 3. 88
1000 225390	+1,0	-0,050	1000,000 43	12. 4. 84
			1000,000 46	21. 11. 84

* In terms of $R_K = 25\,812,8092$

** $R_t = R_{20} + \alpha(t/^\circ\text{C} - 20) + \beta(t/^\circ\text{C} - 20)^2$

the integrating circuit of the FET operational amplifier O71. Integration is initiated by a signal closing the CMOS switch 1 via signals sent along optical fibres, switch 2 being open. After the pre-set integration time, switch 1 is opened, thus stopping integration and holding the result at the output of the O71 for it to be read by the commercial digital voltmeter and reported to the controlling computer via the IEEE 488 data bus. The integrator is reset by closing the CMOS switch 2.

The repeatability and linearity of the integrator is assured by using high-quality insulation for those parts of the circuit associated with the input of the O71, and by selecting the 2 μF integrating capacitor to have high insulation resistance and to exhibit very low dielectric storage. Dielectric storage is responsible for a charged capacitor which has been discharged by shorting, slowly regenerating some fraction of its original charge. If a capacitor exhibiting this effect to a significant degree were used in an integrator, the result would depend on its preceding state. Samples of various capacitor types were investigated [15], and the best individual capacitor selected. This effect then did not cause more than 100 ppm change in the gain or linearity of the integrator for the repeated similar measurements encountered in actual use.

The integration period of 2,3 s was chosen to be the mean of the periods of the two possible simple pendulum motions of the suspended coil on its terminal knife-edge and crossed strip-hinge. In this way, induced voltages caused by a small flux cut, as a result of the alignment procedure described in Sect. 2.2.3 being imperfectly carried out, are averaged over a nearly complete period and reduced to a negligible level.

The linearity and gain of the complete circuit, including the digital voltmeter, was periodically measured by presenting to the input known small dc voltages generated from an accurate 0–1 volt source by a precision resistive attenuator. The source was reversed to eliminate thermal emfs and the offset of the preamplifier. The

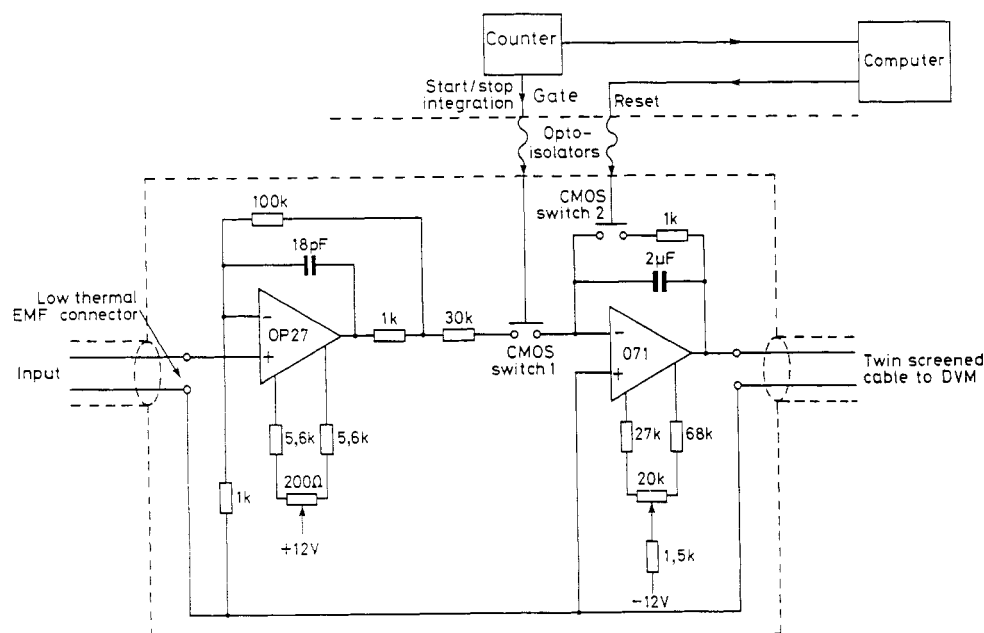


Fig. 8. The circuit of the nanovolt integrator, showing the computer control

small dc voltage was calibrated directly by the Josephson junction array apparatus.

2.2.9. Thermometry, Barometers, Hygrometer and CO₂ Content. This section describes the apparatus necessary to measure the ambient air density (for buoyancy corrections to the weights) and refractive index (to calculate the laser wavelength). The air temperature in the vicinity of the coil is taken to be that of the magnet, which is measured with a calibrated platinum resistance thermometer. The resistance of this thermometer, and that of the thermometer measuring the temperature of the standard resistor is measured with an automatic ac resistance bridge and scanning system [16]. The temperature of the entire apparatus is stabilized by encasing it in a cabin the walls of which are lined with aluminium panels having attached copper pipes through which thermostatically controlled water flows at a rate of one pass every 2 minutes. Therefore the inside surface of the cabin, including walls and ceiling, forms an isothermal surface whose temperature is controlled to 0,1 °C. The 50 mm lagging of the balance and magnet then ensures that their temperature drifts only slowly, at a typical rate of 2 mK/hour. This drift rate corresponds to a change of about 0,4 ppm/hour in the magnetic flux.

The barometric pressure is measured by two precision aneroid barometers. These are calibrated against a standard barometer which has in turn been calibrated against the national primary standard barometer. The pressure readings of the two aneroid barometers are found to have a constant systematic difference of 55 ± 5 Pa, and this gives reassurance as to their continued accuracy between calibrations.

The relative humidity of the air in the cabin is measured with an uncertainty of 2% using a calibrated Assman wet-and-dry bulb hygrometer which, at the end of each measurement run, samples the air in the magnet enclosure by drawing it via a wide tube through the instrument. The instrument can thus be read without the need to enter the cabin.

The CO₂ content of the air in the cabin is measured with an infrared gas analyser which similarly draws a sample of air through a tube from the vicinity of the coil. The instrument is calibrated with CO₂-free nitrogen and with nitrogen containing a certified 400 ppm of CO₂.

All three instruments were calibrated, both directly and indirectly, against instruments which were themselves used in association with an air refractometer.

2.2.10. The Laser Interferometer. The optical configuration of the laser interferometer is that of a conventional Michelson interferometer having corner-cubes as mirrors (Fig. 9). One corner-cube is rigidly fixed to the coil as described above, and the other forms an assembly with the beam-splitter. This assembly is rigidly mounted on the part of the magnet structure which retains a pole-piece, and protrudes into the lowest aperture in the coil former, being then positioned about 150 mm below the corner-cube attached to the coil. The laser itself is mounted remotely outside the cabin containing the apparatus to avoid convection currents being generated by the heat it

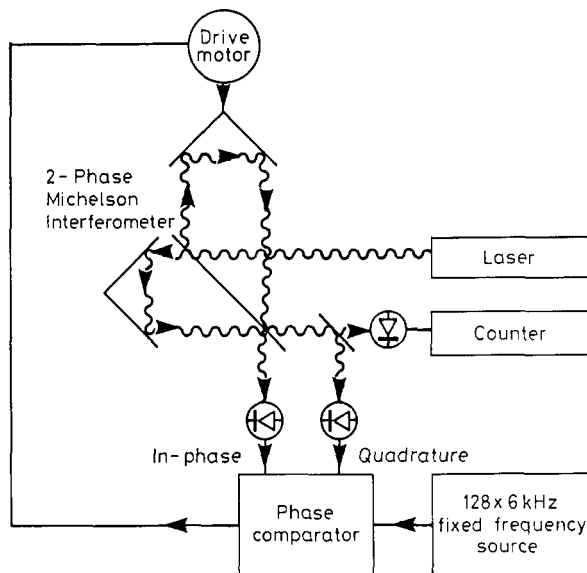


Fig. 9. The scheme for servo-controlling and measuring the velocity

dissipates and the laser frequency being perturbed by the stray flux of the magnet.

Three He-Ne wavelength-stabilized lasers, a Hewlett-Packard type 5500C, a Spectra Physics type 115 and a Zeeman-effect stabilized laser of NPL design were used successively with two velocity control and measurement systems. Only the last, and most satisfactory, system is described here. It was used for the 1987/88 measurements.

The phase-splitting beam splitter system provided two sets of interfering beams whose resulting fringes were 90° out of phase [8]. The phase difference between the passage of fringes and a fixed-frequency source was detected using a circuit [9] which could track this difference over $\pm 16 \pi$ radians. This phase difference was linearly converted to a current which was fed to the drive motor coil G attached to the coil support column (Fig. 4). Coil G lies in the annular gap of the magnet assembly N. In this way a mean velocity constant to within about 10 ppm is maintained over the ± 15 mm of the coil motion about the position the coil occupies for the weighing with the balance beam horizontal. Adjustable gain and damping were provided so that the system could minimize the perturbations due to external vibrations.

The system also counts bi-directionally, the passage of fringes so that the interferometer could measure coil displacement, as a means of keeping the balance in equilibrium for all force determinations.

The correctness of measurement of the coil velocity by the earlier systems was verified by an experiment in which light from a totally independent laser was simultaneously sent through the interferometer. The returning beams from the fixed and moving corner-cubes were combined on a light-sensitive diode and the passage of orthodox optical fringes observed. When displayed on an oscilloscope simultaneously with the input to the counter, excellent coherence of phase was observed between the two signals. Also, V/u measurements were carried out consecutively using the two signals as inputs to the counter in turn. The result is discussed in Sect. 3.3.6.

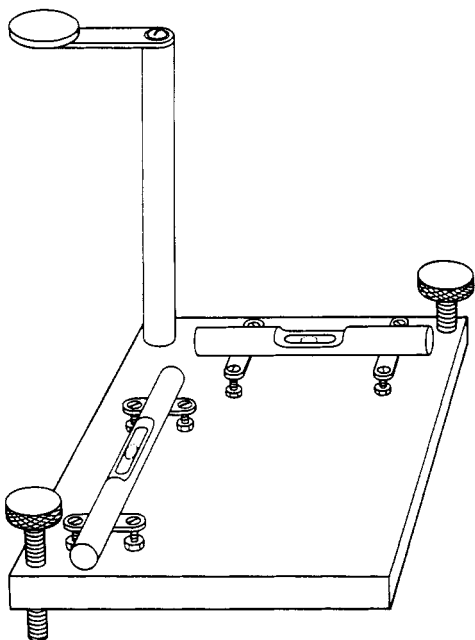


Fig. 10. The mirror and bubble-level apparatus for ensuring the verticality of the laser beam

The frequencies of the three lasers used for the measurements were measured with negligible uncertainty in terms of an iodine-stabilized He-Ne laser at intervals during their use for these measurements.

It is vital to the accuracy of the measurements that the interferometer light beam going to and from the corner-tube attached to the coil should be vertical, as otherwise a cosine error is incurred in the velocity measurement. This adjustment is accomplished with the aid of a small plane mirror interposed in the way of the returning beam so as to reflect it back towards the laser. Bubble levels and levelling screws on the base of the mirror mounting assembly, which is illustrated in Fig. 10, enable the mirror surface to be set in a horizontal plane, the reading of the levels for this condition having been pre-determined by looking down simultaneously on the mirror and a mercury pool with a sensitive autocollimator. With the mirror in position and the levelling screws adjusted to reproduce the required level indications, the direction of the laser beam entering the interferometer is adjusted until it is coincident with the beam returning through the system from the mirror. In this way, the laser beam in the interferometer can be adjusted to be vertical to an accuracy of 10^{-4} rad.

2.2.11. Computer Control. Only the system used in the 1987–1988 measurements is described; that used previously involved only the HP 9825 computer without an auxiliary computer but its operation did not differ materially from that used later.

At the beginning of each day's work the auxiliary computer can, via the velocity control system, move the coil so that the light repeatedly traverses the photocells. In this way the horizontal condition of the balance beam as described in Sect. 2.2.2. is recorded as an interferometer fringe reading. The current flowing in D (Fig. 3 b) is

then a measure of the mass needed on the right side of the balance to restore equilibrium with no current in D. This mass is added by means of the tetrahedral weights described in Sect. 2.2.2. Daily adjustment is necessary to account for the change in mass of the coil which is probably caused by changes in the ambient relative humidity altering the water content of the tufnol former.

The measurement of the voltage induced in the moving coil begins with the velocity servo system (Sect. 2.2.10.) manipulating the current to D to traverse the coil up and down repeatedly. The velocity of the coil is measured by the counter over a succession of very short time intervals until the desired value of about 2 mm/s is achieved. The velocity-measuring fringe counter is activated and a step voltage signifying the opening of its gate starts the integrating voltmeter. Removal of this voltage 2,38 s later, on closing the gate of the counter, stops the integrator. The held output of the integrator is read by a digital voltmeter which then reports to the computer the observed average difference, over this interval, between the voltage induced in the coil and the voltage standard. The counter measures in fringes per second the mean velocity over this interval. Simultaneously, the 9825 computer receives distance information from the interferometer in order to ascribe a mean position to these observations.

When the coil is travelling upwards the state of the reversing switch to the voltage standard is changed. About fifteen up and down traverses constitute a complete measurement of the voltage/velocity ratio. The results of a typical measurement are shown in Fig. 11 a, where a parabola has been fitted by the least-squares method to the experimental points. Evidently the fit to the expected smooth variation of the flux distribution through the moving coil is good. The position corresponding to a horizontal balance beam is the zero abscissa and is marked as a vertical broken line. The required result of the measurement is the interpolated ratio of velocity to voltage at this position. In Fig. 11 b the data has been re-plotted as deviations from best-fit parabolae to show the random scatter in more detail. The coil moving upwards gives rise to the left-hand groups of + points and the coil moving downwards to the right-hand groups of ● points.

In the weighing measurement, illustrated schematically in Fig. 3 a, an isolated current source controllable with 0,2 ppm resolution by an auxiliary computer supplies current to the coil. The auxiliary computer controls this current so as to keep the balance beam at rest in the horizontal position (as recorded by the displacement readings of the laser interferometer). One of two algorithms is used. These are (i) a fast-acting acceleration-nulling routine used while masses are being raised or lowered and (ii) a slower acting displacement and velocity-damped routine which maintains equilibrium and thereby stabilizes the current for measurement. The auxiliary computer also deduces from the distance readings of the laser interferometer when the balance is steady with the beam horizontal and the current can be measured. The 9825 computer is left free to receive the results from the integrating voltmeter, which now measures the voltage difference between the potential drop of the equilibrium

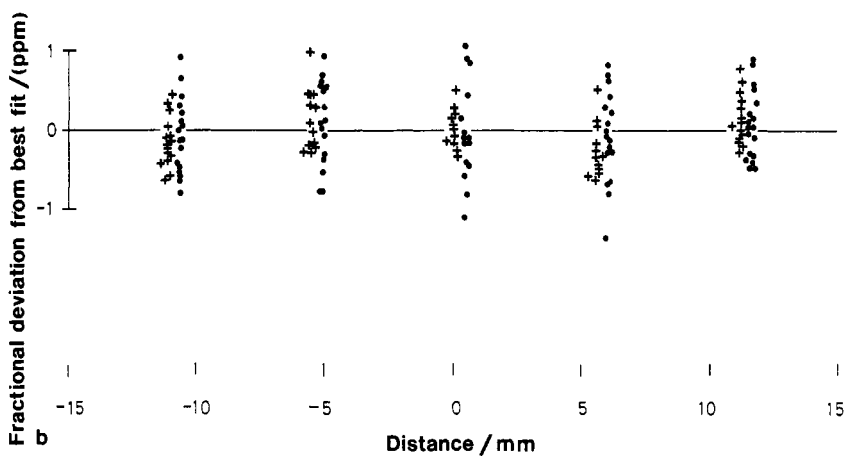
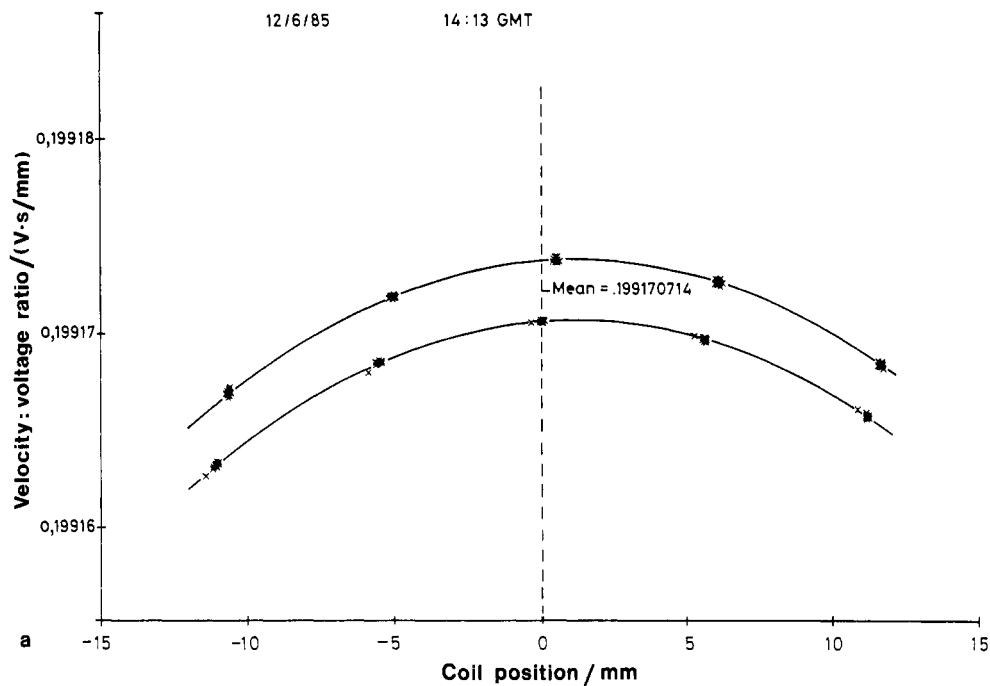


Fig. 11 a, b. The result of a V/u determination

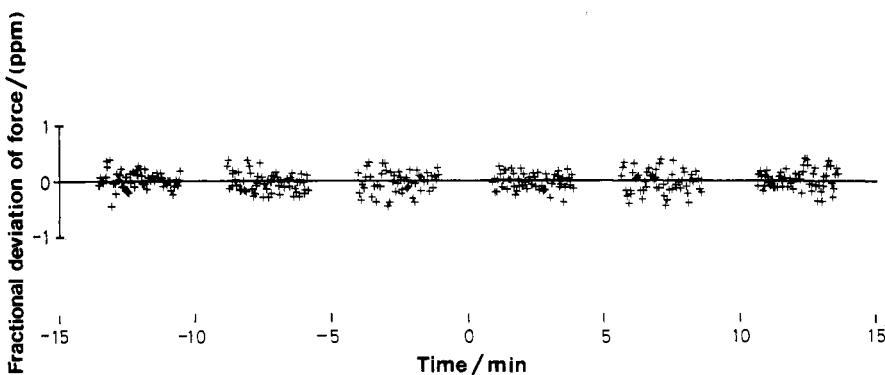


Fig. 12. The result of a force determination

current flowing through the standard resistor R and the emf of the standard voltage source. At the end of a set of readings it operates the weight lowering and raising mechanism and the voltage source reversing switch.

Some typical observations obtained as the masses on the left of the balance case were lowered and raised three

times are shown in Fig. 12. The clusters of plotted points each correspond to 60 observations of the output of the integrating voltmeter obtained at 2,38 s intervals with the left-hand mass either lowered or raised. The data has been reduced for this graphical presentation by subtracting the fitted ordinates occurring at the mean time of the

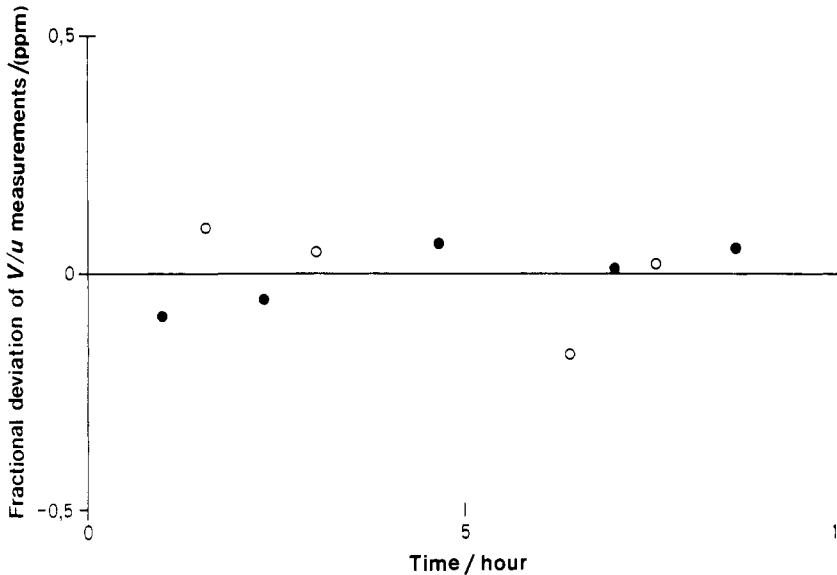


Fig. 13. A set of results constituting a measurement

complete weighing operation and the common slope of the least-squares fitted lines through the three data clusters corresponding to each state of the mass. The common slope reflects the drift of the balance. At the mean time of the complete sequence, half the difference of the ordinates for each mass state, when added to the voltage of the standard voltage source, constitutes the result of the weighing measurement.

About four velocity/voltage measurements interleaved with weighings are carried out during the course of a day's observations. A typical set is plotted as a function of time in Fig. 13 where the common slope of the weighing and velocity-voltage measurements caused by the drift in magnetic flux has been subtracted. The auxiliary data needed to calculate a result, namely the temperature of the air in the optical path of the interferometer (assumed equal to the magnet's temperature), the barometric pressure, humidity and CO₂ content, the temperature of the standard resistor and the day's value of the voltage standard in terms of the NPL maintained volt are taken at intervals and linearly interpolated to the mean times of the velocity and weighing measurements.

2.2.12. Computational Algorithms. Six computational algorithms are required to specify the condition of the air in the experimental chamber. They describe air pressure, temperature, relative humidity, CO₂ content, density and refractive index.

a) Total air pressure. The total air pressure p is measured with two calibrated precision aneroid barometers. Their temperature coefficient is negligible over the small range of laboratory temperatures encountered. They are positioned at the same height as the laser interferometer, rather than the height of the masses as the buoyancy correction is much smaller. Corrections are applied and the mean taken.

b) Air temperature. The air temperature t is measured with a platinum resistance thermometer calibrated at 20°C. The manufacturer's data was taken to calculate

dt/dR for a $\pm 1^\circ\text{C}$ range about 20°C. The resulting temperature accuracy is better than $5 \times 10^{-3}^\circ\text{C}$.

c) Relative humidity. The relative humidity, r , is measured with a forced-air wet-and-dry bulb hygrometer. Its value, expressed as a percentage, is calculated from an empirical expression which applies when the air temperature is about 20°C;

$$r = [96,5 - 7,45 (\text{dry bulb temperature} - \text{wet bulb temperature})] \% .$$

The molar fraction of water vapour, x_v is calculated from Ref. [17], equation (19)

$$x_v = (r/100) f(p, t) p_{sv}(t)/p ,$$

where $p_{sv}(t)$ is the saturation vapour pressure of water at temperature t and the enhancement factor $f(p, t)$ is taken as 1,004 to a sufficient approximation for the range of p and t encountered. Similarly the algorithm

$$p_{sv}(t) = [2339 + 145(t/^\circ\text{C} - 20)] \text{ Pa} ,$$

is taken as fitting the data of Table 2 of this reference well enough for our purpose.

d) CO₂ content of the air. The CO₂ content of the air, x_c , is measured with an infra-red absorption instrument, calibrated with CO₂-free N₂ and a 400 ppm by volume CO₂-N₂ mixture.

e) Density of the air. The algorithm of Ref. [17], equation (16) is used.

$$\rho_{\text{tphx}} / \text{kg} \cdot \text{m}^{-3} = [3,483\ 53 + 1,44 \times 10^{-6} (x_c - 400)] \cdot (1 - 0,378\ 0\ x_v) 10^{-3} p/ZT$$

where Z is the 'compressibility factor' for moist air, which we take as 0,9996 for the range of p and t encountered. The thermodynamic temperature is T , equal to $t + 273,15$ K.

f) Refractive index of the air. The refractive index of air, n_{tph} , is calculated for the 633 nm laser wavelength from

the formula given in Ref. [18], page 86, as revised by Birch and Downs [19],

$$n_{\text{tph}} = 1 + \{0,000\,276\,517\,6[1 + (61,3 - t/^{\circ}\text{C}) \times 10^{-10} p/\text{Pa}] / 96\,095,4(1 + 0,003\,661\,t/^{\circ}\text{C}) - 3,635 \times 10^{-10} x_v\} p/\text{Pa}$$

A correction for the typical CO₂ content of the air is made as +15 ppb * per 100 ppm by volume of CO₂ content: above 300 ppm by volume CO₂ content, the correction is calculated according to the information given in Ref. [20], equation (5).

3. Errors

To assess the relative sizes of errors more easily, and to avoid decimal fractions, all fractional errors and uncertainties are here expressed as parts in 10⁹, that is, in parts per billion. ‘Negligible’ errors are defined as those less than 10 ppb.

3.1. Type A (Random) Errors

Type A, or random, errors are defined as those contributing to the variation in the result of one determination from another carried out in as identical conditions as possible.

3.1.1. Random Error Associated with V/u Measurement. The irreducible limit of precision is set by Johnson noise, the only significant contributions to which arise from the 100 Ω resistance of the coil and the 1000 Ω internal resistance of the voltage standard. Johnson noise is therefore about 4 nV Hz^{-1/2}, or about 3 nV since the integrating time of the digital voltmeter is 2,38 s. This is negligible, and is much less than the other random uncertainties to be discussed.

The noise of the integrating voltmeter is dominated by that of the OP27 preamplifier stage (Fig. 8), and the standard deviation of a single 2,38 s integration is observed to be about 30 ppb. It is difficult to quantify exactly as repeated observations of the output are subject to slow variations due to changing thermal emfs, 1/f noise and the rectification of residual radiofrequency interference.

The voltage reference sources have a similar short-term variability of less than 50 ppb and a longer term variation from hour-to-hour (linear drift having been accounted for) of up to 50 ppb about a mean value. Figure 7 shows a typical record of the stability of the voltage source over a period of a few hours, which is the time taken for one determination. Usually two or more measurements of the voltage standard, in terms of standard cells, were carried out during the measurements. These values indicated that our voltage standard typically changed by less than 50 ppb during a measurement period.

Cutting of flux by the coil due to motions other than the required vertical motion introduces spurious voltages in the V/u determination. This effect was minimized by the procedure described in Sect. 2.2.3. For a ‘pendulum’

swing of the coil of 10⁻³ rad the induced voltages at the fundamental frequency and first harmonic are less than 100 μV peak-to-peak. When a measurement is in progress the swing of the coil is less than 5 × 10⁻⁵ rad and so the maximum expected peak-to-peak voltage is less than 5 μV. This is integrated over a complete period to within 2% and therefore the residual ‘noise’ from this cause is less than 0,1 μV or 100 ppb. Torsional oscillations about a vertical axis of 10⁻² rad generate less than 7 mV peak-to-peak. When making measurements these oscillations are less than 3 × 10⁻⁵ rad, so that the induced voltage then is less than 21 μV. As the period of torsional oscillations is 0,67 s, about 6,5 oscillations occur in the integration time, leading to about 1,7 μV of peak-to-peak ‘noise’. Therefore torsional oscillations are likely to be the predominant cause of random noise in the V/u measurement. As the ordinate at a given abscissa on the mean best-fit parabola (Fig. 11 a) results from the order of 60 observations the random error of determining the ordinate at the weighing position can be expected to be established with about 30 ppb precision.

3.1.2. Random Error Associated with Weighing. Johnson noise, integrating voltmeter noise, noise from the voltage reference source and electrical interference are about the same as for the V/u determination. Voltages introduced by unwanted motions of the coil ought not to introduce noise as the current to the coil is supplied by a very high impedance current source. The noise of the latter is about 100 ppb Hz^{-1/2}, and, when averaged by the long time-constant of the servo-controlled balance, is negligible. The dominant sources of noise arise from the finite resolution of the laser distance readings (0,3 μm) leading to steps in the current demanded by the servo-controlling algorithm, mechanical vibration and tilting of the building. Figure 12 shows a typical set of weighing observations. A common slope and the mean difference between alternate groups of points, which correspond to alternate positioning and raising of the kilogram mass, have been subtracted. It will be seen that each group of 60 points comprising an observation has a standard error of the mean of about 0,03 μV. The scatter of the set of six groups representing three successive positionings and raisings of the mass about a straight line is larger, being typically 0,1 μV or less, because of non-linear drifts. The causes of these include disturbance of the balance on raising or repositioning the mass. The overall weighing random error is about 30 ppb for observations made with a 1 kg mass, to which must be added the 50 ppb random variations of the standard voltage source to give an expected ± 60 ppb variability in the weighing observations.

The coil will warm slightly whilst current is passing during the weighing. With 10 mA passing for a typical 20 min during a weighing sequence, the temperature rise is about 1 mK and the linear expansion of the coil dimensions would be 17 ppb. This effect would produce a negligible contribution to the drift in the results during a measurement sequence.

3.1.3. Drift During a Measurement Cycle. A sequence of alternating weighings and V/u determinations is carried

* 1 ppb = 1 × 10⁻⁹

out to eliminate, by linear interpolation, the effect of various drifts. The flux density of the magnet alters due to its changing temperature, the coil dimensions alter and the refractive index and density of the air change. The results of weighing and V/u measurements change typically by 500 ppb per hour, making interpolation to the nearest minute necessary to cause negligible error. Fortunately, drift is sufficiently linear over the few hours a measurement takes. Figure 13 shows a set of results constituting a measurement taken on a day when the drift rate was somewhat higher than usual. The standard deviation of a point from the fitted line is about 170 ppb. The random error of a determination of K_V , which is the ratio of the maintained voltage unit defined in terms of the Josephson frequency-to-voltage conversion ratio of 483 594 GHz/volt (maintained) to the SI volt, is about 60 ppb from this data. This random error includes the random errors associated with the auxiliary measurements of barometric pressure, air temperature, relative humidity and CO₂ content, of adjustment of the laser beam in the interferometer to be vertical, and of relating the standard voltage source to the Josephson apparatus. The complete 1σ random uncertainty associated with each watt realization is listed in Table 4, and drawn as error bars in Fig. 15.

3.1.4. The Random Standard Error of the Mean of the 1987–1988 Measurements. Assuming $R_K = 25\,812,809\,2\ \Omega$, the weighted mean of the 1987–1988 measurements is $\Delta K_V = -8,070\ \text{ppm}$,

(where $K_V = 1 + \Delta K_V$) with a total random error of the mean of 24 ppb.

3.2. Type B Errors

Under the heading of Type B, or anticipated systematic, errors we consider those influences for which corrections are calculated from supplementary observed parameters using algorithms established beyond doubt by the work of others.

These systematic errors are summarised in Table 3. A – entry signifies an error of less than 10 ppb, contributing negligibly to the overall root sum-of-squares error.

Half of the root sum-of-squares of the errors in Table 3 (excluding the voltage measurement errors) is 31 ppb in terms of a defined R_K value, or 41 ppb in terms of $R_{K,NPL}$ obtained by including the * item in the table. These figures when combined with the voltage measurement error and the 24 ppb standard error of the mean of all 1987–1988 results give a total error of 68 ppb or 73 ppb respectively.

Whereas the coil occupies a definite position for the force measurement, the V/u data are sampled over a 5 mm distance per point so a correction must be made for the curvature of the V/u parabola about the force measurement position over this distance. This correction is 504 ppb on the V/u data, and is subject to negligible error. The validity of this correction was verified experimentally by taking data sampled over a 10 mm distance per point and observing the apparent shift in the parabola.

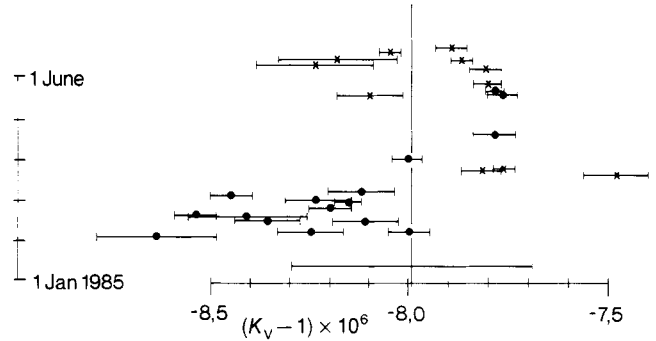


Fig. 14. The 1985 results

Table 3. Type B (systematic) errors

Source of error	Error/ppb
<i>Associated with voltage measurement</i>	
Realisation of the maintained Josephson volt at NPL	–
Calibration of standard cells maintaining V_{NPL} from above	30
Calibration of our voltage standard from above cells or direct from the Josephson array	40 50
Thermal emfs in our voltage standard reversing switch	–
Calibration of the gain of the nanovolt integrator	<25
Root sum-of-squares	56
<i>Associated with the resistance standards</i>	
Measurement of the SI value of R_K	54*
Relating our 100 Ω standards to $R_{K,NPL}$	10
Temperature corrections to our 100 Ω standards	–
Ageing and resulting interpolation or extrapolation	–
Load coefficients of resistors	–
<i>Associated with the masses</i>	
The NPL 1 kg standard in terms of the 1 kg prototype	10
Our 1 kg and other masses in terms of the NPL standard	10
<i>Associated with gravitational acceleration</i>	
Determination of g in SI units at NPL Teddington 'A' site	10
Difference in g between 'A' and the position of our masses	10
Tidal corrections to g	–
<i>Associated with the velocity measurement</i>	
Laser wavelength in vacuum from an I_2 stabilized laser (limited by laser stability)	10
Measurement of the optical fringe frequency	20
<i>Associated with atmospheric refractive index, n, and density</i>	
Atmospheric pressure, uncertainty 10 Pa. (Error of 27 in n)	–
Atmospheric temperature, uncertainty 5 mK. (Error of 5 in n)	–
Atmospheric relative humidity, uncertainty 2%. (Error of 20 in n)	–
Atmospheric CO ₂ content, uncertainty 20%. (Error of 10 in n)	–
Error in n arising from these uncertainties	35
Error in n from calculational formula	33
Error in buoyancy correction to masses arising similarly (Strongly correlated with the error in n)	20
<i>Associated with geometrical alignment</i>	
Laser beam imperfectly vertical in the interferometer	–
Gaussian (non-planar) wavefront of the laser	–
Imperfectly flat optical components	10
Rotation of the corner-cube	–

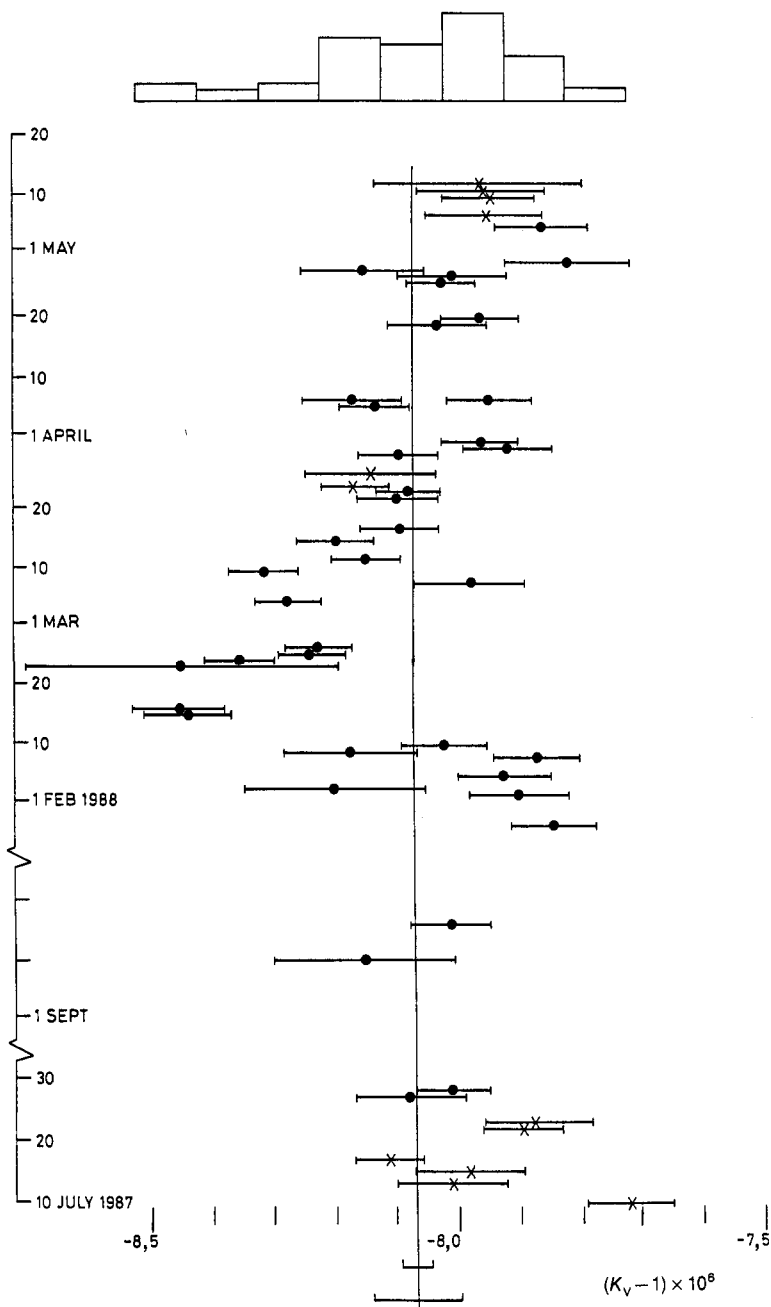


Fig. 15. The 1987–1988 results. The smaller error bar at the bottom of the diagram represents the standard error of the mean of these 50 watt realizations and the lower, larger error bar results from combining this with the uncertainties of known causes of systematic error

3.3. Search for Other Systematic Errors

3.3.1. Coil Misalignment. In principle, the measurement should be independent of the alignment of the coil in the magnetic field so long as the rate of change of the flux threading the coil with vertical displacement at the position it occupies for the force measurement is the same as when it moves through that position in a vertical direction for the V/u measurement. In practice it is clearly desirable that the change in flux threading the coil with displacement or rotation in other directions is minimized, which we did using the method described in Sect. 2.2.3. To verify experimentally the above statement, measurements were made with the coil deliberately misaligned. No change in the result, outside random error was found.

3.3.2. Force Measurement with a Non-horizontal Balance Beam. A problem arises if there is any significant force on the coil in the plane of the balance beam, due to imperfect magnetic alignment. Such a force exerts a couple on the beam via the terminal knife-edge supporting the coil and the central knife-edge. This couple reverses with current direction and therefore causes an error in the force measurement. To show experimentally that the alignment procedure of Sect. 2.2.3 is adequate, force measurements were performed when the line joining these knife-edges departed from horizontal by about ten times the usual adjustment tolerance. No significant effect was found.

3.3.3. Force Measurement with the Coil in Different Positions up a Vertical Line. As shown in Fig. 2, the balance

is supported on an hydraulic lifting column which enables it and the coil to be raised or lowered with respect to the magnet. By this means, force measurements can be made at various positions along the trajectory of the coil when it moves. In this way it was verified that the parabolic variation of the flux threading the coil with coil position is also observed for the force measurement.

3.3.4. The Effect of Simple and Torsional Pendulum Motions of the Coil. In the course of the observations conditions sometimes occurred in which simple and torsional pendulum motions of the coil were considerably in excess of the usual residual amounts. The results of the V/u or force measurements made under these conditions were not significantly different except in so far as the apparent noise was increased.

3.3.5. Measurements Made with Different Currents. It is most important to discover whether there were any effects due to the interaction of the current in the coil with the magnetic circuit. These effects should be eliminated by reversal of the current and observation of the force change due to this reversal. To test this, measurements were made with nominal values of the current of 1, 5 and 10 mA corresponding to masses of 0,1, 0,5 and 1 kg respectively. A single current of 1 mA was used in the 1985 results. The 1987–1988 results grouped in this way are summarised in Table 4.

In order to test whether the current flowing in the coil during force measurement alters the state of the permanent magnet appreciably and thereby influences the subsequent V/u determination, measurements were made in which a current of 20 mA – twice the maximum current usually used – was passed through the coil, and a shift in the value of V/u was sought immediately afterwards. A shift was found which correlated with the direction in which the current flowed in the coil and, assuming this shift to be approximately linear with the current, a correction of about 100 ± 50 ppb was applied to the 1985 results obtained with 1 kg mass and 50 ± 25 to the results obtained with 0,5 kg mass. For the 1987–1988 results, the final current direction of a weighing was equally distributed in sign and, on examination of the individual force and V/u measurements comprising a realization, no significant systematic effect was found.

The mean of the results obtained with 1 kg mass differs from the mean of those obtained with 0,5 kg mass. A t-test reveals that there is only a 3% chance that the means of the 5 mA and 10 mA results differ by the observed amount or more, but this becomes a 5% chance if data from the period (15–24). 2. 1988 are ignored.

3.3.6. Measurements Made with Different Velocities. Using the standard voltage source which had two 0,509 V outputs in series, V/u data was obtained for each of the 0,509 V sections separately and for the total voltage. The value obtained for the last measurement was, within random error, equal to the average obtained for the two 0,509 V sections separately. Measurements made against the Josephson array apparatus verified that the sum of

the two 0,509 V outputs equalled the 1,018 V output to 10 ppb.

The variation of V/u with position of the coil in the magnetic flux is a curve which ought to be dependent only on the flux distribution. We found that this curve, which is a parabola to within the accuracy of the data, had a very slightly different curvature depending on whether the data corresponded to the coil ascending or descending. Several possible causes of this were investigated. For example, the coil might take a slightly different path according to whether it was moving down or up, and the flux threaded might depend significantly on the path taken. So we took data when the coil was deliberately displaced a relatively large amount from the experimentally determined symmetrical position. The curvature discrepancy of this data was identical to that obtained with the undisplaced alignment.

The fringe-counting system of the laser interferometer is another possible cause, and measurements made with a separate stabilized laser and fringe detection system gave different curvature anomalies definitely associated with the deterioration in interferometer alignment as the balance beam departed from a horizontal condition during coil movement. The same V/u value was obtained as with the usual system however, so we concluded that this small systematic effect is unimportant. A careful elimination of residual digital noise from the laser display being picked up by the voltage measurement circuit appeared to improve this effect. For the 1987/1988 data the fringe-sensing photodetector, which measures the coil velocity, was physically and electrically separated from the digital equipment except for the one connection to the input of the counter. No further problems of digital interaction were expected or observed.

3.3.7. Input Offset Current of the Nanovolt Integrator. A V/u measurement performed with a 15 k Ω resistor connected in series with the standard voltage source showed a symmetric displacement of the results as the coil moved up and down. The displacement amounted to +30 ppm, but the mean differed from measurements obtained with the resistor shorted by only 200 ppb. The displacement is caused by the 2 nA input offset current of the preamplifier of the nanovolt integrator. Since the output impedance of the two standard voltage sources used in these measurements were 1 k Ω , 1,2 k Ω and 1,5 k Ω any systematic error from this cause ought to be negligible.

3.3.8. Simulation of Poor Coil Insulation. No exceptional care was taken over the internal insulation of the coil windings as leakage should affect the V/u and force measurements by an equal and opposite amount, an advantage conferred by the ‘virtual work’ nature of the principle of the measurement. This reasoning was tested by connecting a 5 M Ω resistor across the windings of one half of the coil and performing a measurement. The result was, as expected, not affected by the presence of the resistor.

3.3.9. Other Insulation of the Electrical Circuit. The insulation of various parts of the electrical circuit from each other and from the all-enclosing electrical shield were measured and found in general to be in excess of $10^{11} \Omega$. Where possible, the conductors, switches, isolated power supplies etc. were insulated with PTFE or similar low-conductivity plastic materials, but the coil was supported from the balance with tufnol and the insulation to the screen here was only of the order of $10^{11} \Omega$. As an additional check, results were obtained with the connections to the coil, standard voltage source, integrator and (for weighing) the current source reversed. For the 1985 results, small systematic effects of 150 ppb were found. The mean of the two conditions was assumed to be correct and a correction of (75+75) ppb made. For the 1987–1988 results, this effect could not be substantiated and no correction or uncertainty allowance was made.

3.3.10. Magnetic Field Gradients Acting on the Masses. A small permanent magnet was placed in the balance case adjacent to the kilogram mass in such a position as to produce a magnetic field gradient in the vertical direction of 50 times that usually present. Removal or replacement of this magnet had no significant effect on the balance equilibrium, whether the kilogram mass was lowered into position or not.

3.3.11. Coil Permeability. Because the measurement method makes no assumptions about the actual flux density, the alteration of that originally present by the small but finite magnetic permeability of the coil ought to be immaterial. This hypothesis was tested by performing one measurement with a sheet of paper attached to the side of the lower half of the coil structure. The paper was coated with varnish loaded with colloidal iron particles. The effect of this shim was to alter the flux density by a fraction $1,2 \times 10^{-5}$. The result of the measurement with the shim attached was, within random error, the same as the others.

4. Conclusions

4.1. Results and Implications

The results obtained in 1985 are plotted in Fig. 14.

The results obtained on various dates during 1987–1988 for various values of the masses are summarised in Table 4 and plotted in Fig. 15. The uncertainties associated with the individual realizations are 68% confidence intervals estimated from 1) the scatter of the weighing and V/u data comprising the realization of K_v , as in the example of Fig. 13, combined with 2) the other known and quantifiable causes of random variation between realizations. These are ± 18 ppb for the random component of the refractive index calculation from the measured barometric pressure, air temperature, relative humidity and CO_2 content, ± 10 ppb from the same causes of variability in ascertaining the buoyancy correction on the masses, an allowance of ± 10 ppb for the possibly

Table 4. Results of individual realizations carried out in 1987–1988, assuming $R_K = 25\,812,809\,2$

Date	$\Delta K_v \times 10^6$	Uncertainty $\sigma(\Delta K_v) \times 10^6$	Current/mA	
10. 7. 87	-7,722	0,069	5	
13. 7. 87	-8,015	0,089	5	
15. 7. 87	-7,986	0,090	5	
17. 7. 87	-8,117	0,054	5	
22. 7. 87	-7,899	0,064	5	
23. 7. 87	-7,878	0,082	5	
27. 7. 87	-8,081	0,089	10	
28. 7. 87	-8,014	0,060	10	
10. 9. 87	-8,154	0,146	10	
16. 9. 87	-8,013	0,064	10	
28. 1. 88	-7,845	0,069	10	
2. 2. 88	-7,900	0,078	10	
3. 2. 88	-8,202	0,146	10	
5. 2. 88	-7,924	0,075	10	
8. 2. 88	-7,870	0,069	10	
9. 2. 88	-8,175	0,108	10	
10. 2. 88	-8,022	0,071	10	
15. 2. 88	-8,441	0,069	10	
16. 2. 88	-8,455	0,074	10	
23. 2. 88	-8,452	0,256	10	
24. 2. 88	-8,356	0,055	10	
25. 2. 88	-8,240	0,053	10	
26. 2. 88	-8,230	0,054	10	
4. 3. 88	-8,282	0,052	10	
7. 3. 88	-7,981	0,090	10	
9. 3. 88	-8,320	0,055	10	
11. 3. 88	-8,154	0,055	10	
14. 3. 88	-8,203	0,062	10	
16. 3. 88	-8,097	0,063	10	
21. 3. 88	-8,100	0,066	10	
22. 3. 88	-8,081	0,052	10	
23. 3. 88	-8,170	0,055	5	
25. 3. 88	-8,144	0,106	5	
28. 3. 88	-8,097	0,064	10	
29. 3. 88	-7,918	0,074	10	
30. 3. 88	-7,964	0,062	10	
5. 4. 88	-8,134	0,056	10	
6. 4. 88	-7,948	0,069	10	
6. 4. 88	-8,171	0,081	10	
18. 4. 88	-8,032	0,082	10	
19. 4. 88	-7,962	0,063	10	
25. 4. 88	-8,024	0,054	10	
26. 4. 88	-8,007	0,088	10	
27. 4. 88	-8,153	0,100	10	
28. 4. 88	-7,817	0,102	10	
4. 5. 88	-7,858	0,078	10	
6. 5. 88	-7,954	0,095	5	
9. 5. 88	-7,947	0,074	5	
10. 5. 88	-7,959	0,103	5	
11. 5. 88	-7,963	0,170	5	
	Combinations of results			
	All 50	5 mA	1987	Omitting period 15. 2. 88 to 24. 2. 88
Mean	8,070	7,979	7,988	8,038
Std. deviation	0,167	0,125	0,127	0,133
Std. error of mean	0,024	0,036	0,040	0,020

imperfect adjustment of verticality of the laser beam in the interferometer and ± 30 ppb for relating our standard voltage source to the Josephson array apparatus.

It is clear from Table 4 that the known causes do not account for all the observed variation in the individual realizations, particularly during the period from 10. 2. 88 to 10. 5. 88, but it is important to note that these realizations are not mere repetitions without alterations in the measurement conditions. On the contrary, as many changes as possible were made, such as re-alignments of the optical path through the interferometer, changing the type of frequency-stabilized laser used, reversing connections in the measurement circuit of Fig. 6, realignments with varying degrees of precision of the coil in the flux, as noted in Sect. 3.3.1, and readjustment of the mass centre of the coil assembly. We have no reason to suppose that the mean value arising from any or all of these adjustments is other than zero, and so no systematic uncertainty allowance is made for them in the final estimated uncertainty.

The mean of the 1987/1988 measurements, $\Delta K_V = (-8,070 \pm 0,073)$ ppm is the same as the $\Delta K_V = (-8,00 \pm 0,3)$ ppm result obtained for the 1985 measurements, Fig. 14, to well within their combined uncertainties. Because of the much smaller uncertainty ascribed to the 1987–1988 results, and many minor improvements to the apparatus and experimental technique since 1985, no account has been taken of the 1985 results in arriving at the result reported here.

The working unit of voltage has hitherto been maintained in terms of a Josephson effect apparatus by ascribing the value 483 594 GHz/volt (maintained) to the Josephson constant presumed to equal to $2e/h$ exactly. The measurements reported here suggest the value $(483\,597,903 \pm 0,035)$ GHz/V ought to be used, based on the premise that the SI value of the quantum Hall resistance is $R_K = 25\,812,809\,2\,\Omega$. If we also presume that $R_K = h/e^2$ exactly, since $e = 2/(R_K K_J)$, we find that $e = (1,602\,176\,35 \pm 0,000\,000\,14) \times 10^{-19}$ C.

This result may be compared with the CODATA recommended value [5].

Also, in the equation

$$h = 4/(K_J^2 R_K),$$

the dimension of resistance is eliminated, so the direct transfer of a resistor between the quantum Hall apparatus and the moving-coil apparatus obviates the need to include the uncertainty associated with the realization of the ohm from the calculable capacitor. Therefore we obtain

$$h = (6,626\,068\,21 \pm 0,000\,000\,90) \times 10^{-34} \text{ J s}.$$

This result has a quarter of the uncertainty of the value we reported previously [4].

Since 1972, following the recommendation [2] by the Comité Consultatif d'Électricité of the Comité International des Poids et Mesures, a value of $K_J = 483\,594,0$ GHz/V has been used by most national laboratories for disseminating the SI volt by calculation of standards of voltage [14]. There is now ample evidence [21]

that this value of K_J is some 8 ppm in error. Our measurements and those of other laboratories have provided data for this committee, enabling it to recommend a revised value of $K_J = 483\,597,9$ GHz/V and a value of $R_K = 25\,812,807\,\Omega$ to be used from 1 January 1990 to derive reference standards for the volt and ohm respectively.

4.2. Future Outlook – Prospects for Re-defining the Kilogram

Assuming that the systematic errors described in Sect. 3.3.6 (half-voltage, half-velocity measurements) and Sect. 3.3.9 (coil etc. reversed) are more fully investigated and either eliminated or accounted for, the next dominant error figure arises from the calibration of our laboratory voltage standard in terms of the NPL Josephson effect apparatus. This error figure would need to be reduced to 30 ppb or less to reduce the overall error significantly.

Assuming that our voltage standard could be related to a Josephson multi-junction array with less than 5 ppb uncertainty, together with the presently achievable 5 ppb uncertainty for calibrating our resistors in terms of the quantum Hall effect, and that air refractive index and buoyancy corrections were eliminated by putting the apparatus in a vacuum, one might achieve 10 ppb uncertainty with which to define a 'kilogram' in terms of the Josephson and quantum Hall effects [22].

Acknowledgements. We are grateful to: Mr R. C. Smith for constructing much of the apparatus and software, Mr P. Spreadbury of the Engineering Laboratory, Cambridge University, for supplying us with one of the standard voltage sources, Mr K. Birch (NPL) for checking that our barometers, hygrometer and CO₂ content meter gave the correct result for the refractive index of air as measured by a refractometer. Mr D. Simpson (NPL) for calibrating our barometers. The mass calibration section of NPL for calibrating our masses, Dr W. R. C. Rowley (NPL) for calibrating our laser frequency, and for the loan of a frequency-stabilized laser, Dr A. Hartland and Mr N. B. Dupuy (NPL) for calibrating our resistors, Dr R. G. Jones and Mr D. R. Smith (NPL) for measuring our voltage standards against the NPL Weston cells, and Mr P. J. Krause and Mrs L. A. Henderson (NPL) for measurements against the Josephson multi-junction array apparatus. Mr Richardson (Imperial College Geophysics Dept.) for relating 'g' to British fundamental gravity station, Prof. Sakuma (BIPM) for tidal corrections to g, Mr K. W. Raine (NPL) for making the phase-separating optical beam-splitter, and the many others within and outside NPL who contributed to the success of these measurements.

References

1. R. G. Jones, B. P. Kibble: IEEE Trans. Inst. Meas. **IM34**, 181–184 (1985)
2. BIPM Com. Cons. Electricité, **13**, 1972: Declaration E-72, pp. E13–E14
3. A. Hartland, R. G. Jones, D. J. Legg: Document CCE/88-9 submitted to the 18th meeting of the CCE, 1988
4. B. W. Petley, B. P. Kibble, A. Hartland: Nature **327**, 605–606 (1987)
5. E. R. Cohen, B. N. Taylor: Rev. Mod. Phys. **59**, 1121–1148 (1987)
6. B. P. Kibble: in: *Atomic Masses and Fundamental Constants 5*. J. H. Saunders, A. H. Wapstra, eds., (Plenum Press, New York 1976) pp. 541–551

7. B. P. Kibble, I. A. Robinson: *Feasibility study for a moving-coil apparatus to relate the electrical and mechanical SI units*. NPL Report DES 40, 1977
8. M. J. Downs, K. W. Raine: *Precision Engineering* **1**, 85–88 (1979)
9. I. A. Robinson: *A Many Cycle Phase Detector Applied to an Interferometer for Velocity Control*. (In preparation)
10. B. P. Kibble, G. J. Hunt: *Metrologia* **15**, 5–30 (1979)
11. B. P. Kibble, G. J. Hunt: NPL Divisional Report QU 15, 1971
12. B. P. Kibble, I. A. Robinson: *An isolated mains-driven power supply*. NPL Memorandum DES 54, 1985
13. A. Hartland, T. J. Witt, D. Reymann, T. F. Finnegan: *I.E.E.E. Trans. Inst. Meas.* **IM-27**, 470–474 (1978)
14. P. J. Krause, A. Hartland: 1 volt Josephson voltage standard using series arrays of tunnel junctions. B.E.M.C. Digest (NPL Publication 1987) pp. 13/1–13/5
15. C. C. Casey, I. A. Robinson, B. P. Kibble: *Dielectric storage in capacitors used in precise integrating circuits*. NPL Memorandum DES 47, 1983
16. I. A. Robinson: Thesis submitted for the Ph.D degree of University College, University of London (1988)
17. P. Giacomo: *Metrologia* **18**, 33–40 (1982)
18. G. W. C. Kaye, T. H. Laby: *Tables of Physical and Chemical Constants*, 14th ed, (Longman, London 1973) p. 86
19. K. P. Birch, M. J. Downs: *J. Phys. E.* **21**, 694–695 (1988)
20. F. E. Jones: *J. Res. Nat. Bur. Std.* **86**, 27–32 (1981)
21. B. N. Taylor: *IEEE Trans. Inst. Meas.* **IM36**, 659–664 (1987)
22. B. P. Kibble: in: *Precision Measurements and Fundamental Constants II*, B. W. Taylor, W. D. Phillips, eds., Natl. Bur. Stand. (U.S.) Spec. Publ. 617, (1984), pp. 461–464